WARPED S-TRANSFORM FOR ANALYSING THE BRAIN WAVES

Adam Borowicz

Faculty of Computer Science, Bialystok University of Technology, Białystok, Poland

Abstract: In this paper the warped S-transform is introduced as a tool for non-uniform time-frequency representation (TFR) of the brain electrical activity. The brain oscillations are classified as the five basic rhythms. The center frequencies and frequency ranges of these rhythms are non-uniformly distributed over frequency scale. Unlike the conventional S-transform the proposed technique is based on the warped discrete Fourier transform (WDFT), that allows for frequency scale warping. This can improves a spectral resolution of the TFR in particular oscillation band. In opposition to the time-domain filtering techniques, the brain rhythms can be analysed more precisely in the time-frequency plane as a full-band signal.

Keywords: WDFT, Stockwell transform, EEG

1. Introduction

The use of electro-encephalography (EEG) for registering brain activity has gained growing interest in recent years. Five simple periodic rhythms recorded in the EEG are *alpha*, *beta*, *gamma*, *delta* and *theta*. Since these rhythms are related to different brain activities they are usually analysed independently. Most commonly, the signals within the delta band ($<$4 Hz) correspond to a deep sleep, theta frequencies (4-8 Hz) are typical for dreamlike state, alpha band (8-13 Hz) signals correspond to relaxed state, beta band (13-35 Hz) is related to waking activity and gamma frequencies ($>$ 35 Hz) are characteristics for mental activities [3]. It should be noted that those are the basic rhythms only and the full classification of the brain waves includes slow ($<$1.5 Hz), fast and ultra fast waves ($>$80 Hz). An important brain wave is also *mu* rhythm that is commonly used as a control feature for brain-computer interfaces (BCIs) [8]. The *mu* oscillations (7.5–12.5 Hz) occupies the same frequency range as the *alpha* rhythm but specifically, they occur in the sensorimotor (SM) cortex.

Advances in Computer Science Research, vol. 11, pp. 5-16, 2014.

Unfortunately, the exact mechanisms of most brain oscillations are not known. Some oscillations are independently generated, but many of them are active simultaneously. Therefore it is usually assumed that the frequency content of the EEG recordings is non-stationary and multicomponent.

The discrete Fourier transform (DFT) is widely used in spectral analysis. It provides global information about the amplitude and phase spectra of the signal at each frequency. However the EEG recordings (due to its non-stationary nature) are better described by time-frequency representations (TFRs). Short-time Fourier transform (STFT) was one of the first TFR technique [16]. Its major disadvantage is inability to obtain a good frequency and time resolution of low and high frequency events at once. In order to overcome this limitation the S-transform has been proposed [19]. In opposition to the STFT, it employs a variable window length providing better time-frequency resolution. The S-transform is similar to a continuous wavelet transform (CWT) [4] but in opposition to the CWT the amplitude and phase spectra of the S-transform are directly related to the spectra of the Fourier transform. It has found applications in many fields including the EEG data analysis [15], [14].

Those methods are powerful tools in uniform spectral analysis. However the center frequencies and the frequency ranges of the popular oscillation bands are non-uniformly distributed over linear frequency scale. Some studies [12] indicate that, they rather form a geometric progression on the linear scale (and a linear progression on a natural logarithmic scale). Therefore the uniform spectral analysis of the full-band EEG signal may not be the best choice. Usually, in order to analyse particular brain wave the EEG signal is filtered using time-domain methods [11]. However in this case, some important signal features can be lost or not visible enough (in time domain). On the other hand some studies suggest [8], [10] that amplitude/phase coupling exists between two or more oscillation bands. Thus, the non-uniform TFR technique that is able to increase spectral resolution in arbitrarily selected oscillation band while the preserving the full-band information can be interesting alternative.

A typical example of the non-uniform frequency decomposition tool is warped discrete Fourier transform (WDFT) [9]. Number of the WDFT applications can be found in the literature of signal processing, including filter banks [9] and frequency estimation [5]. The WDFT was also employed in perceptual speech enhancement [13], [2].

In this article a warped S-transform is introduced as a tool for non-uniform time-frequency analysis of the brain wave EEG recordings. The proposed technique is based on the WDFT and allows for an improving frequency resolution in particular oscillation band at cost of the lower resolution in other bands. We propose to use second order allpass function to obtain a proper frequency scale warping. In oppo-

sition to the time-domain filtering methods, the warped S-transform is strictly TFR technique thus the all bands can be analysed at once on the time-frequency plane.

2. The S-Transform

The continuous S-transform [19] of the function $x(t)$ is defined as follows

$$S(\tau, f) = \int_{-\infty}^{\infty} x(t) g(\tau - t, f) e^{-i2\pi f t} dt, \tag{1}$$

where τ and f denote the time variable and Fourier frequency, respectively and $g(t, f)$ is a Gaussian window

$$g(t, f) = \frac{|f|}{\sqrt{2\pi}} e^{-(tf)^2/2}. \tag{2}$$

The frequency domain definition of the discrete S-transform, for $n = 0, 1, ..., N-1$ and $k = 1, 2, ..., N-1$ is given by

$$S\left[n\Delta, \frac{k}{N\Delta}\right] = \sum_{m=0}^{N-1} X\left[\frac{k+m}{N\Delta}\right] e^{-2\pi^2 m^2/k^2} e^{i2\pi mn/N}, \tag{3}$$

where Δ denotes sampling interval and $X\left[\frac{k}{N\Delta}\right]$ is the DFT of the N-point time series $x[m\Delta]$ (with $m = 0, 1, ..., N-1$). For $k = 0$ and any n the S-transform is simply equal to arithmetic mean of $x[m\Delta]$, i.e.

$$S[n\Delta, 0] = \frac{1}{N} \sum_{m=0}^{N-1} x[m\Delta]. \tag{4}$$

The TFR is strictly redundant, the inverse of the S-transform can be computed using inverse DFT of the time-averaged spectra, i.e.

$$x[m\Delta] = \sum_{k=0}^{N-1} \frac{1}{N} \sum_{n=0}^{N-1} S\left[n\Delta, \frac{k}{N\Delta}\right] e^{i2\pi km/N}. \tag{5}$$

There are computational advantages that come from using the frequency domain definition (3). Namely it can be implemented using the fast Fourier transform (FFT) algorithm.

3. The WDFT definition

The WDFT is not in itself the TFR technique, it transform the one-dimensional sequence of the time domain samples to one-dimensional frequency domain representation. It can be considered as a special case of non-uniform discrete Fourier transform [1]. In the case of the WDFT, the frequency samples are allocated non-uniformly but regularly over the unit circle. For the sequence $x[n]$ of the length N, it is defined by

$$\hat{X}[z_k] = X[\hat{z}_k] = \sum_{n=0}^{N-1} x[n]\hat{z}_k^{-n},\ k = 0,1,...,N-1, \tag{6}$$

with $\hat{z}_k$ being the images of allpass transformed equidistant points of the unit circle

$$z_k^{-1} = e^{-i2\pi k/N} \rightarrow \hat{z}_k = A(z_k^{-1}), \tag{7}$$

where $A(z)$ can be an arbitrary, stable allpass function. As a generalization of the DFT, the WDFT maintains some of its properties related to the linearity, symmetry and shifting [9], [5]. Unfortunately, certain important properties are lost.

The matrix representation of the WDFT is given by

$$\begin{bmatrix} \hat{X}_0 \\ \hat{X}_1 \\ \vdots \\ \hat{X}_{N-1} \end{bmatrix} = \underbrace{\begin{bmatrix} 1 & \hat{z}_0^{-1} & \dots & z_0^{-N+1} \\ 1 & \hat{z}_1^{-1} & \dots & z_1^{-N+1} \\ \vdots & \vdots & \ddots & \vdots \\ 1 & \hat{z}_{N-1}^{-1} & \dots & z_{N-1}^{-N+1} \end{bmatrix}}_{\mathbf{D}} \begin{bmatrix} x_0 \\ x_1 \\ \vdots \\ x_N - 1 \end{bmatrix}, \tag{8}$$

with $\hat{X}_k$ denoting $\hat{X}[z_k]$ and x_k denoting $x[k]$. This representation is also a basis for computation inverse transform. The matrix $\mathbf{D}$ is in fact the Vanermonde matrix and for distinct points $\{z_k\}_{k=0}^{N-1}$ its inverse is guaranteed from the theoretical point of view. Note that the elements of the WDFT matrix are no longer the roots of unity, thus the construction of fast computation algorithm like the FFT, seems impossible. The currently fastest algorithm was proposed in [9]. It exploits the factorization of the WDFT matrix into the product of the three matrices: real, the DFT (implemented via the FFT) and complex diagonal one. Its complexity is significantly reduced, but still of $O(n^2)$.

4. Warped discrete S-transform

The TFR-based version of the WDFT can be implemented using a sliding-window technique in a similar manner as the STFT. However due to fixed window length a

such technique allows only for a rough time-frequency representation and is rather dedicated to real-time processing applications. Therefore we propose a novel TFR technique that is rather based on the S-transform and exploits some WDFT features.

The discrete S-transform can be defined for points on a complex plane $\{z_k\}_{k=0}^{N-1}$ as follows

$$S[n\Delta, z_k] = \sum_{m=0}^{N-1} x[m\Delta] g_k(n\Delta - m) z_k^{-m}, \tag{9}$$

where

$$g_k(n\Delta - m) = g\left(n\Delta - m, \frac{\arg z_k}{2\pi}\right). \tag{10}$$

The warped discrete S-transform can be considered as a special case of the non-uniformly sampled continuous S-transform. Similarly to (6), it can be obtained from (9) by replacing z_k with $\hat{z}_k$, i.e.:

$$\hat{S}[n\Delta, z_k] = S[n\Delta, \hat{z}_k]. \tag{11}$$

Unfortunately we can not use the frequency domain definition similar to (3) and the FFT algorithm, thus the computational advantages are lost. Instead we propose to use a vector/matrix notation which can be more suitable for hardware implementation on some platforms. Let $\mathbf{x} = [x[0]\, x[\Delta] \ldots x[(N-1)\Delta]]^T$ be an input vector and $\hat{\mathbf{s}}_k = [\hat{S}[0, z_k]\, \hat{S}[\Delta, z_k] \ldots \hat{S}[(N-1)\Delta, z_k]]^T$ be a corresponding S-transformed vector for kth spectral bin. It can be verified that

$$\hat{\mathbf{s}}_k^T = \left(\mathbf{D}_{\{k,:\}} \otimes \mathbf{x}^T\right) \mathbf{G}_k, \tag{12}$$

where $\mathbf{D}_{\{k,:\}}$ denotes kth row of the WDFT matrix, $\otimes$ is Kronecker product and

$$\mathbf{G}_k = \begin{bmatrix} g_k(0) & g_k(1) & \ldots & g_k(N-1) \\ g_k(1) & g_k(0) & \ldots & g_k(N-2) \\ \vdots & \vdots & \ddots & \vdots \\ g_k(N-1) & g_k(N-2) & \ldots & g_k(0) \end{bmatrix}, \tag{13}$$

is a symmetric Toeplitz matrix composed from Gaussian window coefficients. From (12) we can derive

$$\mathbf{x}^T = \left(\hat{\mathbf{s}}_k^T \mathbf{G}_k^{-1}\right) \otimes \mathbf{D}^*_{\{k,:\}},\ k > 0, \tag{14}$$

which can be viewed as the inverse transformation. This expression is rather not surprising since the time-frequency representation is redundant. Also note that for some $k << N-1$ the signal is highly averaged, thus the matrix $\mathbf{G}_k$ can be ill-conditioned.

5. Adjusting the allpass function to the brain waves

The allpass function of the warped S-transform is determined by particular application. In the case of the brain waves spectral analysis, we propose to increase frequency resolution within a specific oscillation band. It can be done by appropriate adjustment of the allpass filter parameters that results in squeezing/compressing the z-transform points on a particular section of the unit circle. Although there is some control over the behaviour of the first-order allpass filter [5], more control is afforded using the second-order allpass filter, whose the transfer function is given by [17]

$$A(z) = \frac{a_2 + a_1 z^{-1} + z^{-2}}{1 + a_1 z^{-1} + a_2 z^{-2}}, \tag{15}$$

where a_1, a_2 are real valued parameters. For stability reasons we assume $|a_m| < 1$ for all m. In order to ensure a proper mapping range, for $k = 0, 1, ..., N/2$, we propose to use a modified allpass function

$$\hat{z}_k = \hat{A}(z_k^{-1}) = A(z_k^{-1} e^{i\phi}) e^{i\theta}, \tag{16}$$

where $0 < \theta < \pi$ determines the location on unit circle where the frequency samples are concentrated and ϕ is a phase offset. In our discussion we assumed that N is even, for simplicity. Thus the z-transform points, for $k = N/2 + 1, ..., N - 1$, can be computed according to

$$\hat{z}_k = \hat{A}^*(z_{N-k}^{-1}). \tag{17}$$

It can be verified that (16) is in itself a complex allpass function

$$\hat{A}(z) = \frac{\alpha_2^* + \alpha_1^* z^{-1} + \alpha_0^* z^{-2}}{\alpha_0 + \alpha_1 z^{-1} + \alpha_2 z^{-2}}, \tag{18}$$

with

$$\begin{aligned} \alpha_0 &= e^{-i(\theta/2 - \phi)}, \\ \alpha_1 &= a_1 e^{-i\theta/2}, \\ \alpha_2 &= a_2 e^{-i(\theta/2 + \phi)}. \end{aligned} \tag{19}$$

Similarly to the first-order allpass function [5], the magnitude of the parameter α_2 (i.e. a_2) determines the local resolution and can be viewed as the independent variable. For example, for $a_2 = 0$, all frequency samples are placed uniformly on the unit circle, whereas for $0 < a_2 < 1$ the frequency samples are compressed around the point $e^{i\theta}$. We found it empirically that the parameter a_1 together with ϕ controls phase mapping range. In order to cover entire Nyquist frequency range (from 0 to π) we assume that

$$\begin{cases} \hat{A}(e^{i0}) = e^{i0} = 1 \\ \hat{A}(e^{i\pi}) = e^{i\pi} = -1 \end{cases} \tag{20}$$

Since the parameters a_2 and θ are given, we can solve above equation set for a_1 and ϕ. As a result we obtain

$$\phi = \arg z_c, \;\; a_1 = \frac{a_2^2 - 1}{|z_c|}, \tag{21}$$

with $z_c = a_2 e^{-i\theta} - e^{i\theta}$. Thus, the only thing we have to do is to adjust the parameters a_2 and θ, for a particular oscillation band. As mentioned before, the parameter a_2 controls the strength of the frequency scale warping, whereas the parameter θ corresponds to the warping location on the unit circle. Therefore we propose to set

$$\theta = 2\pi f_c / f_s, \tag{22}$$

and

$$a_2 = \frac{1 - \tan(\pi f_b / f_s)}{1 + \tan(\pi f_b / f_s)}, \tag{23}$$

where f_s is a sampling rate and f_c, f_b is respectively the center frequency and bandwidth of the selected oscillation band. It can be verified that (23) is inversely proportional to the bandwidth f_b, thus for narrower bands we get stronger warping. In fact the equation (23) is commonly used to adjust 3dB attenuation bandwidth of notch filters [17].

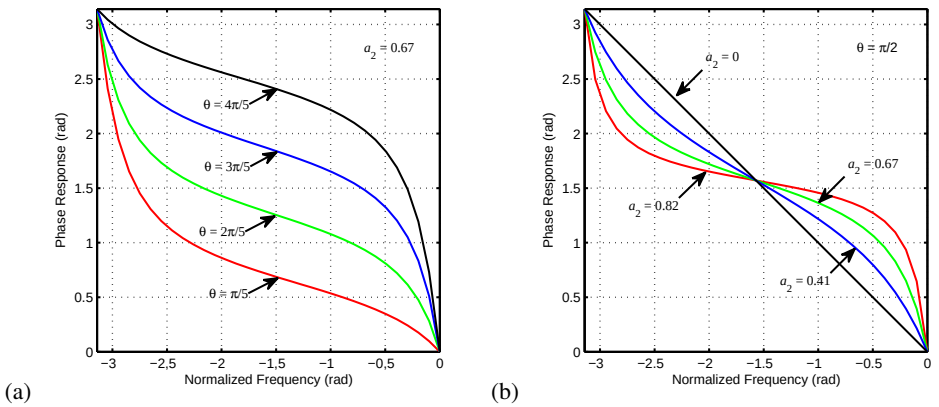

Fig. 1. Adjusting the phase responses of the modified allpass filter: (a) illustrates how the frequency warping location can be adjusted by varying a parameter θ, while (b) illustrates how the warping strength can be tuned by varying a_2.

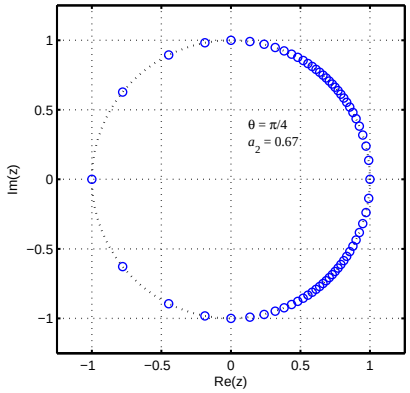

Fig. 2. Locations of the allpass-transformed points $\{\hat{z}_k\}_{k=0}^{N-1}$ on the unit circle.

In Figure 1 we depicted phase responses of the modified allpass filter (16), for different values of the parameters θ and a_2. Figure 2 presents the locations of the allpass-transformed points on the unit circle, for $\theta = \pi/4$, $a_2 = 0.67$ and $N = 64$.

The proposed TFR technique has also been verified using real EEG data. The recordings have been selected from PhysioNet database [6], [18]. They contain the brain activity related to different motor/imagery tasks (opening and closing either both fists or both feet). The EEG data were recorded at 160 Hz sampling rate from 64 electrodes placed according to the international 10-10 system [7] (excluding electrodes Nz, F9, F10, FT9, FT10, A1, A2, TP9, TP10, P9, and P10). For our purposes we selected the signal from electrode C3 (placed above SM cortex of the left hemisphere). The *mu* waves are present when SM cortex is in the idle state and they are suppressed when subject performs or imagines a motor action.

Figure 3a presents the spectrogram obtained using conventional S-transform with uniform frequency scale. The spectrograms presented in Fig. 3b and Fig. 3c have increased spectral resolution within the *beta* and *mu* band respectively. They have been both obtained using warped S-transform for parameters $f_c = 10$ Hz, $f_b = 5$ Hz (*mu* band) and $f_c = 24$ Hz, $f_b = 22$ Hz (*beta* band). As can be seen the time-frequency plane is non-uniformly stretched (warped) along the Y-axis. Note that the strongest stretch is around the center frequency of a given oscillation band. In other words the spectral resolution decreases with increasing distance from the center frequency. Thus we can analyse the selected brain wave in details while preserving some signal features of the full-band activity. For instance, in Fig. 3c although the warped

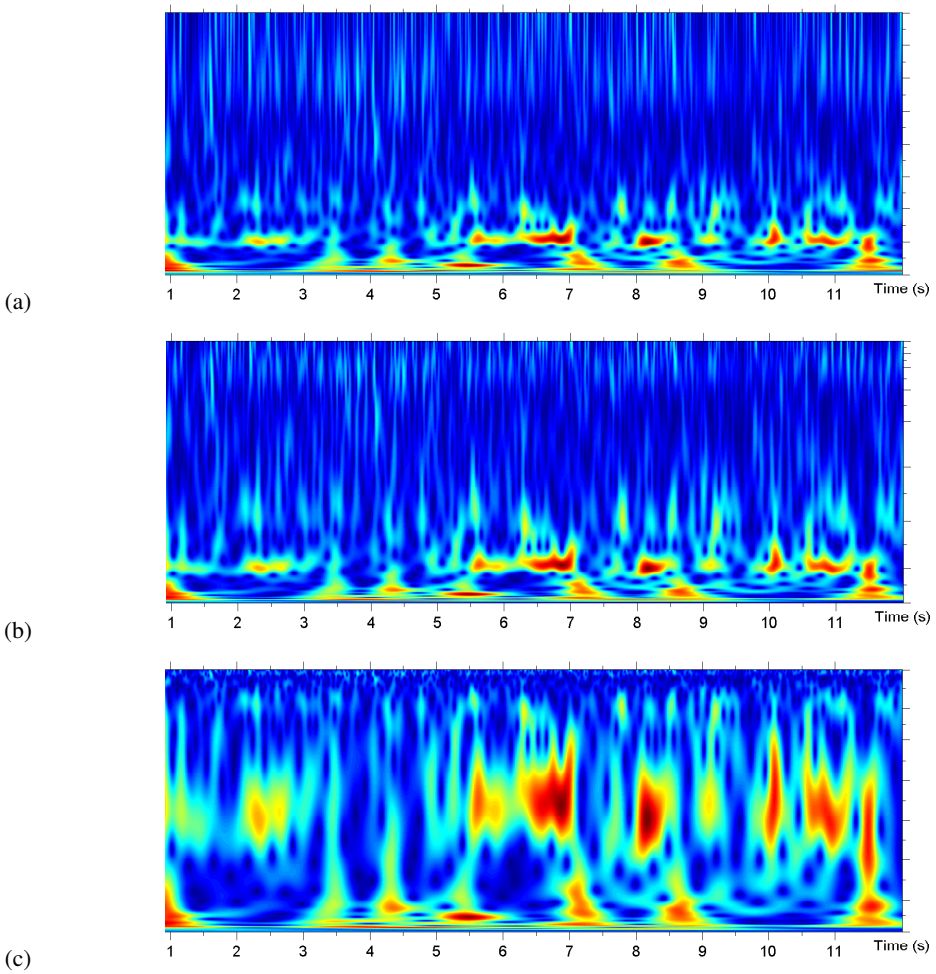

Fig. 3. Spectrograms of the example EEG signal recorded at electrode C3, obtained using: conventional S-transform (a), warped S-transform adjusted to reveal activity in *beta* (b) and warped S-transform tuned to *mu* band (c).

S-transform has been tuned to *mu* band, some activities in *beta* and lower bands are still visible.

In the case of relatively large bandwidths the deformation of the frequency scale is rather small, thus the Fig. 3b does not introduce much information comparing to Fig. 3a. Otherwise, for relatively narrow oscillation bands (i.e. *mu* rhythm) the time-frequency components are visualised in details. It should be noted that the increase in spectral resolution comes from data interpolation. In fact true frequency resolution depends only on window size. However by relocating transform points on a unit circle we can minimize spectral leak in a particular oscillation band and some spectral components can be more visible.

6. Summary

We have introduced the warped S-transform as non-uniform TFR technique for analysis of the brain waves. In fact the novel approach can be considered as a special case of the continuous S-transform with non-uniformly sampled frequency bins. In order to achieve a proper frequency scale warping we exploited the allpass function of the second order in a similar manner as in the case of the WDFT-based methods. The expressions for allpass function parameters have been provided that allows for adjusting the frequency scale warping to a particular oscillation band. It results in stretching the time-frequency plane along the Y-axis and around the center frequency of the selected brain wave. In this way, the rhythms can be better visualized on a time-frequency plane. At the same time by representing the full-band signal, we retain information about relationships between different bands.

Acknowledgment

This work was supported by the Polish National Science Centre under Decision No. DEC-2012/07/D/ST6/02454.

References

[1] S. Bagchi and S.K. Mitra. The nonuniform discrete fourier transform and its applications in filter design. i. 1-d. *Circuits and Systems II: Analog and Digital Signal Processing, IEEE Trans. on*, 43(6):422–433, Jun 1996.

[2] A. Borowicz, M. Parfieniuk, and A. Petrovsky. An application of the warped discrete fourier transform in the perceptual speech enhancement. *Speech Comm.*, 48(8):1024–1036, 2006.

[3] G. Buzsáki. *Rhythms of the Brain*. Oxford University Press, Inc., New York 2006.

[4] I. Daubechies. The wavelet transform, time–frequency localization and signal analysis. *IEEE Trans. Inf. Theory*, 36:961–1005, 1990.

[5] S. Franz, S.K. Mitra, and G. Doblinger. Frequency estimation using warped discrete fourier transform. *Signal Process.*, 83(8):1661–1671, Aug 2003.

[6] A. L. Goldberger, L. A. N. Amaral, L. Glass, J. M. Hausdorff, P. Ch. Ivanov, R. G. Mark, J. E. Mietus, G. B. Moody, C.-K. Peng, and H. E. Stanley. PhysioBank, PhysioToolkit, and PhysioNet: Components of a new research resource for complex physiologic signals. *Circulation*, 101(23):e215–e220, 2000 (June 13).

[7] V. Jurcak, D. Tsuzuki, and I. Dan. 10/20, 10/10, and 10/5 systems revisited: Their validity as relative head-surface-based positioning systems. *NeuroImage*, 34(4):1600 – 1611, 2007.

[8] D.J. Krusienski, G. Schalk, D.J. McFarland, and J.R. Wolpaw. A μ-rhythm matched filter for continuous control of a brain-computer interface. *IEEE Trans. Biomed. Eng.*, 54(2):273–280, 2007.

[9] A. Makur and S.K. Mitra. Warped discrete-fourier transform: Theory and applications. *IEEE Trans. Circuits Systems I*, 48(9):1086–1093, 2001.

[10] L.F. Márton, L. Bakó, S.T. Brassai, and L. Losonczi. Multichannel {EEG} signal recording analysis based on cross frequency coupling method. *Procedia Technology*, 12(0):133 – 140, 2014.

[11] J.B. Nitschke, G.A. Miller, and E.W. Cook. Digital filtering in eeg/erp analysis: Some technical and empirical comparisons. *Behavior Research Methods, Instruments, & Computers*, 30(1):4–67, 1998.

[12] M. Penttonen and G. Buzsaki. Natural logarithmic relationship between brain oscillators. *Thalamus and Related Systems*, 2(2):145–152, 2003.

[13] A. Petrovsky, M. Parfieniuk, and A. Borowicz. Warped DFT based perceptual noise reduction system. In *Proc. AES 116th*, Berlin, Germany, May 2004, 14 p.

[14] C.R. Pinnegar, H. Khosravani, and P. Federico. Frequency phase analysis of ictal eeg recordings with the s-transform. *Biomedical Engineering, IEEE Trans. on*, 56(11):2583–2593, Nov 2009.

[15] Kok-Kiong Poh and P. Marziliano. Analysis of neonatal eeg signals using stockwell transform. In *Engineering in Medicine and Biology Society, 2007. 29th Annual International Conference of the IEEE*, pages 594–597, Aug 2007.

[16] M. Portnoff. Time-frequency representation of digital signals and systems based on short-time fourier analysis. *IEEE Trans. Acoust. Speech Signal Process.*, 28(1):55–69, 1980.

[17] P.A Regalia, S.K. Mitra, and P.P. Vaidyanathan. The digital all-pass filter: a versatile signal processing building block. *Proceedings of the IEEE*, 76(1):19–37, Jan 1988.

[18] G. Schalk, D.J. McFarland, T. Hinterberger, N. Birbaumer, and J.R. Wolpaw. Bci2000: A general-purpose brain-computer interface (bci) system. *IEEE Trans. on Biomedical Engineering*, 51(6):1034–1043, 2004.

[19] R. G. Stockwell, L. Mansinha, and R. P. Lowe. Localization of the complex spectrum: the s transform. *Sig. Process., IEEE Trans. on*, 44(4):998–1001, Apr 1996.

SPACZONA TRANSFORMATA S DO ANALIZY FAL MÓZGOWYCH

Streszczenie: W artykule wprowadzamy spaczoną transformatę S, jako narzędzie nierównomiernej reprezentacji czasowo-częstotliwościowej aktywności elektrycznej mózgu. Oscylacje mózgowe klasyfikowane są, jako pięć podstawowych rytmów. Częstotliwości środkowe oraz zakresy odpowiadające tym rytmom rozmieszczone są nierównomiernie na skali częstotliwości. Proponowana technika, w przeciwieństwie do konwencjonalnej transformaty S, opiera się na spaczonej dyskretnej transformacie Fouriera, która pozwala na deformowanie skali częstotliwości. Umożliwia to zwiększenie rozdzielczości widmowej reprezentacji czasowo-częstotliwościowej w określonym paśmie oscylacji. W odróżnieniu od klasycznych metod filtracji dziedziny czasu, rytmy mózgowe mogą być dokładniej analizowane w płaszczyźnie czasowo-częstotliwościowej, jako sygnał pełno-pasmowy.

Słowa kluczowe: WDFT, transformata S, EEG

Artykuł zrealizowano w ramach grantu badawczego Narodowego Centrum Nauki nr DEC-2012/07/D/ST6/02454.